

# Bone imaging in prostate cancer: the evolving roles of nuclear medicine and radiology

Gary J. R. Cook<sup>1</sup> · Gurdip Azad<sup>1</sup> · Anwar R. Padhani<sup>2</sup>

Received: 5 May 2016 / Accepted: 21 June 2016 / Published online: 20 July 2016  
© The Author(s) 2016. This article is published with open access at Springerlink.com

**Abstract** The bone scan continues to be recommended for both the staging and therapy response assessment of skeletal metastases from prostate cancer. However, it is widely recognised that bone scans have limited sensitivity for disease detection and is both insensitive and non-specific for determining treatment response, at an early enough time point to be clinically useful. We, therefore, review the evolving roles of nuclear medicine and radiology for this application. We have reviewed the published literature reporting recent developments in imaging bone metastases in prostate cancer, and provide a balanced synopsis of the state of the art. The development of single-photon emission computed tomography combined with computed tomography has improved detection sensitivity and specificity but has not yet been shown to lead to improvements in monitoring therapy. A number of bone-specific and tumour-specific tracers for positron emission tomography/computed tomography (PET/CT) are now available for advanced prostate cancer that show promise in both clinical settings. At the same time, the development of whole-body magnetic resonance imaging (WB-MRI) that incorporates diffusion-weighted imaging also offers

significant improvements for detection and therapy response assessment. There are emerging data showing comparative SPECT/CT, PET/CT, and WB-MRI test performance for disease detection, but no compelling data on the usefulness of these technologies in response assessment have yet emerged.

**Keywords** Prostate cancer · Bone metastases · Bone scan · Positron emission tomography · Single photon emission computed tomography · Whole body magnetic resonance imaging

## Introduction

The skeleton is the second commonest site for metastases from prostate cancer after lymph nodes, and there is an incidence of 65–75 % of skeletal involvement in patients with advanced disease [1]. Skeletal metastases are associated with significant morbidity and skeletal related events; however, effective palliation strategies are available resulting in improvements in overall survival (currently 12–53 months), longer than with most other types of cancer that have metastasised to bone [2]. Management of prostatic bone metastases has a significant impact on health care resources [3].

It is recognised that conventional imaging, including radiographs, computed tomography (CT) and bone scintigraphy (BS), is relatively insensitive and/or non-specific for the diagnosis of skeletal metastases. In addition, commonly used response assessment methodologies, such as response evaluation criteria in solid tumours (RECIST 1.1) [4], do not adequately cater for bone disease response, especially in osteoblastic disease which is the commonest manifestation in metastatic prostate cancer.

✉ Gary J. R. Cook  
gary.cook@kcl.ac.uk

Anwar R. Padhani  
anwar.padhani@stricklandscanner.org.uk

<sup>1</sup> Division of Imaging Sciences and Biomedical Engineering, Department of Cancer Imaging, Clinical PET Centre, St Thomas' Hospital, Kings College London, London SE1 7EH, UK

<sup>2</sup> Paul Strickland Scanner Centre, Mount Vernon Cancer Centre, Rickmansworth Road, Northwood, Middlesex HA6 2RN, UK

Improvements made in detection with modern hybrid and functional methods, including positron emission tomography (PET)/CT, single-photon emission computed tomography (SPECT)/CT, whole-body magnetic resonance imaging (WB-MRI) and PET/MRI, and the relative merits of these methods will be reviewed in this study. However, the ability to provide a timely and accurate assessment of treatment response, so as to maximise the use of successful treatments and minimise exposure to non-effective treatments (and their toxicities), is less well studied by modern imaging techniques. Nevertheless, there are accumulating data that functional or hybrid imaging is likely to offer superior efficacy in therapy assessment, and these aspects will also be discussed.

### Pathophysiology of bone metastases

Spread of prostate cancer to bone is via the haematogenous route, whereby cancer cells initially settle in the bone marrow where they are able to grow in accordance with the “seed and soil” hypothesis originally proposed by Paget [5]. In bone metastases from prostate cancer, there is predominant upregulation of osteoblastic activity leading to the formation of mineralised woven bone, causing the characteristic osteosclerotic appearance on radiographs and CT, but it is recognised that osteoclasts also play an important part in the pathophysiology of the metastatic growth process [6]. A key mechanism of control is tumour cell influence over osteoblast/osteoclast activity, through the expression of cytokines, including the receptor activator of the nuclear factor- $\kappa$ B ligand (RANKL), an activator of osteoclast differentiation. Increased osteoblastic, osteoclastic, and tumour cell activity are not only therapeutic targets but also represent potential targets for imaging. Other altered imagable bone targets include trabecular bone density, neoangiogenesis, bone marrow fat, water and iron content and tumour related macrophages.

### Tumour cells

Abnormal tumour metabolism may be depicted by a variety of PET tracers. For example, increased membrane synthesis that occurs in proliferating tumours is associated with increased accumulation of choline (e.g.  $^{11}\text{C}$  or  $^{18}\text{F}$ -choline tracers) [7], enhanced fatty acid metabolism (e.g.  $^{11}\text{C}$ -acetate) [8] or amino acid transport (e.g. anti-1-amino-3-[ $^{18}\text{F}$ ]fluorocyclobutane-1-carboxylic acid, FACBC or fluciclovine) [9]. Prostate cancer cells typically do not show significant  $^{18}\text{F}$ -fluorodeoxyglucose metabolism unless dedifferentiated and castrate-resistant [10]. Tracers that image specific aspects of prostate cancer cellular

biology include 16beta- $^{18}\text{F}$ -fluoro-5alpha-dihydrotestosterone ( $^{18}\text{F}$ -FDHT) for androgen receptor targeting [11] and prostate-specific membrane antigen labelled with  $^{68}\text{Ga}$  ( $^{68}\text{Ga}$ -PSMA) [12, 13]. Tumour cell infiltration within the bone marrow can also be detected on morphological T1/T2-weighted MRI sequences but can also be detected by diffusion-weighted (DW) sequences; the latter is sensitive to the increased impediment of water molecule motion in hypercellular tissues [14]. In addition, the displacement of normal bone marrow fat by tumour cells and matrix mineralisation can also be detected on gradient-echo imaging sequences which enable the separate imaging of bone marrow water and fat [15, 16].

### Osteoblastic activity

Increased osteoblastic activity leads to an osteosclerotic appearance on radiographs and CT and causes increased accumulation of bone-specific tracers, such as  $^{99\text{m}}\text{Tc}$ -methylene diphosphonate ( $^{99\text{m}}\text{Tc}$ -MDP) (SPECT) or  $^{18}\text{F}$ -fluoride (PET). The high osteoblastic activity in metastases from prostate cancer compared to other tumours means that these methods have traditionally shown good sensitivity. However, an increase in osteoblastic activity frequently occurs in bone metastases responding to treatment and bone-specific tracers may, therefore, be unable to differentiate an increase or new uptake due to osteoblastic healing (flare phenomenon) from an increase/new activity due to progressive disease [17]. Another limitation of using an indirect osteoblastic detection process for detecting metastatic disease includes missing or underestimating the volume of disease that does not incite an osteoblastic reaction.

### Osteoclastic activity

Osteoclasts lead to bone destruction and osteolytic lesions, and whilst this is a less common appearance in prostate cancer, it may be observed on radiographs and CT. The presence of marked osteolysis should prompt histologic reevaluation, because it can indicate the emergence of aggressive prostate cancer variants, which are increasingly seen in the later stages of the metastatic process after several rounds of treatments. Osteoclasts express high levels of the integrin  $\alpha_v\beta_3$  that facilitates adherence of osteoclasts to the endosteal bone surface, promoting resorption. PET and SPECT tracers that were originally designed to target  $\alpha_v\beta_3$  integrin in tumour-related angiogenesis with the arginine–glycine–aspartic acid (RGD) sequence have shown some utility in targeting osteoclastic activity in bone metastases in animal models and humans [18–20].

## Staging

### Bone scans

Due to the low incidence of skeletal metastases in patients with a new diagnosis of low-risk prostate cancer (e.g. PSA < 10 ng/ml, Gleason score < 8, no bone pain), a staging bone scan is not recommended [21], and some have refined risk factors, e.g. PSA < 20 ng/ml, stage < T4 and Gleason < 8 [22]. In those with an increased risk of bone metastases, the bone scan with tracers such as  $^{99m}\text{Tc}$ -MDP has been the commonest method for detecting skeletal involvement [23]. However, it is recognised that it may not detect small bone marrow-based metastases that have not caused a large enough osteoblastic response to be identifiable. For disease limited to the bone marrow, WB-MRI or PET imaging may be more sensitive [24]. Another perceived weakness of bone scans is a lack of specificity as non-malignant skeletal disease may also cause focal uptake of bone-specific tracers, often requiring further correlative morphological imaging (e.g. radiographs, MRI and CT). With modern hybrid imaging, improved characterisation of the causes of bone scan uptake has largely been addressed, such that morphological appearances can help correctly attribute non-malignant scintigraphic uptake, thus improving specificity and reducing the number of equivocal interpretations. This has been shown with  $^{99m}\text{Tc}$ -MDP SPECT/CT in patients with prostate cancer where compared with planar imaging, the number of equivocal lesions dropped from 61 to 8 % with the addition of SPECT/CT [25].

Whilst the flare phenomenon may cause false positives when assessing treatment response (see below), it may be useful in diagnosing bone metastases in new patients who are started on hormone therapy. A second bone scan 6 weeks after commencing hormones may show either new, previously occult lesions, or an increase in uptake in previous equivocal lesions, thereby improving both sensitivity and specificity in detection of skeletal disease [26].

### $^{18}\text{F}$ -fluoride PET

$^{18}\text{F}$ -fluoride was introduced as a bone-specific tracer more than 50 years ago [27] and has uptake mechanisms similar to diphosphonates (e.g.  $^{99m}\text{Tc}$ -MDP) that rely on blood flow and local osteoblastic activity [28]. However, it was not until the improvement in PET scanners in more recent years, that it was possible to take advantage of the superior imaging characteristics compared to bone scintigraphy.  $^{18}\text{F}$ -fluoride shows rapid skeletal uptake and background soft tissue clearance allowing high-quality skeletal imaging as soon as 1 h after injection. These characteristics, combined with superior spatial resolution and tomographic

acquisitions as a routine, improve diagnostic accuracy in patients with prostate cancer compared with bone scan [29]. A prospective study of 44 patients with high-risk prostate cancer showed superiority of  $^{18}\text{F}$ -fluoride PET/CT over  $^{18}\text{F}$ -fluoride PET, bone scan augmented with SPECT and planar bone scan alone, the respective sensitivities, specificities, positive and negative predictive values being reported as PET/CT: PET: BS + SPECT and BS: 100, 100, 100, 100 vs 100, 62, 74, 100 vs 92, 82, 86, 90 vs 70, 57, 64 and 55 % [28]. In a report from the National Oncologic PET Registry in the USA that assessed the effects of  $^{18}\text{F}$ -fluoride PET/CT in prostate cancer, bone metastasis was confirmed in 14 % at initial staging and 29 % in those with suspected first osseous metastasis [30]. The post-imaging plan was revised to treatment in 77 % and 52 % in these respective groups.

### $^{18}\text{F}$ -FDG PET

Despite the widespread utility in most cancers,  $^{18}\text{F}$ -FDG PET appears to have limited sensitivity in detecting skeletal metastases from prostate cancer. Compared with bone scans,  $^{18}\text{F}$ -FDG PET detected 64 out of 100 bone scan positive lesions in patients with a new diagnosis of prostate cancer and only 4 out of 131 in patients receiving hormone deprivation therapy, in whom PSA levels ranged from 499 to 4786 ng/ml [31]. In another study of patients with hormone-resistant disease, only 18 % of bone scan lesions showed accumulation of  $^{18}\text{F}$ -FDG and the authors concluded that lesions show a low glycolytic rate and that other metabolic mechanisms may be more dominant in prostate cancer [32]. It has also been reported that in castrate resistant prostate cancer patients with  $^{18}\text{F}$ -FDG avid metastases, the number and extent of  $^{18}\text{F}$ -FDG avid disease correlates with survival [33].

### $^{18}\text{F}/^{11}\text{C}$ -choline PET

Both  $^{18}\text{F}$ -choline and  $^{11}\text{C}$ -choline probably show similar diagnostic accuracy. Detection of bone metastases in 140 patients has been reported with  $^{11}\text{C}$ -choline. Uptake was seen in both osteoblastic ( $n = 97$ ) and osteolytic lesions ( $n = 43$ ) but with significantly higher SUVmax in osteolytic disease [34]. Another study showed that densely sclerotic lesions (CT Hounsfield Units > 825) did not show  $^{18}\text{F}$ -choline uptake. It was noted that nearly all of these patients had received hormone therapy and the lack of activity was interpreted as being due to a treatment effect resulting in non-viable bone metastases [35].

Most studies have shown a higher diagnostic accuracy for choline PET/CT compared with bone scans for initial staging or specifically in the spine [36–38]. One study

reported a lower sensitivity but higher specificity and a fewer equivocal lesions [39]. In comparison with  $^{18}\text{F}$ -fluoride PET/CT,  $^{18}\text{F}$ -choline has been reported to show a non-statistically significant lower sensitivity (74 vs 81 %), a higher specificity (99 vs 93 %,  $p = 0.01$ ) and no difference in overall accuracy (85 vs 86 %) [40]. Two patients had bone marrow lesions detected with  $^{18}\text{F}$ -choline with a change in management, and although some patients had more lesions detected with  $^{18}\text{F}$ -fluoride, management was not changed in these. A similar comparison between  $^{18}\text{F}$ -choline and  $^{18}\text{F}$ -fluoride by the same group found no statistically significant differences overall in a group of 42 patients but a better specificity for  $^{18}\text{F}$ -choline in a subgroup of patients with suspected recurrence (96 vs 91 %,  $p = 0.03$ ) [41]. As a tumour-specific tracer, choline is able to detect both bone and soft tissue metastases.

### Other PET tracers

In patients with biochemical recurrence of prostate cancer,  $^{11}\text{C}$ -acetate has shown high concordance with bone scans with a sensitivity of 90 % and specificity of 96 % [42]. In an interesting comparison of  $^{18}\text{F}$ -FDHT and  $^{18}\text{F}$ -FDG with CT in patients with castrate resistant prostate cancer, an inverse correlation was reported between uptake of both tracers and CT lesion density. The number of skeletal metastases on CT and both PET methods predicted survival. Uptake of  $^{18}\text{F}$ -FDHT, but not  $^{18}\text{F}$ -FDG, showed an inverse correlation with survival [33].

There is a strong interest in assessing the role of prostate specific membrane antigen (PSMA) targeting tracers for SPECT and PET imaging given that most prostate cancer cells highly overexpress this target. In patients with biochemical recurrence of prostate cancer,  $^{68}\text{Ga}$ -PSMA has shown higher sensitivity in bone and soft tissue disease with greater lesion conspicuity, particularly in bone [12, 43]. An early description of an  $^{18}\text{F}$ -labelled PSMA tracer analogue suggests superiority over bone scan and  $^{18}\text{F}$ -fluoride PET [13], but a formal comparison has not yet been made in a substantive study. Early data also suggest that  $^{68}\text{Ga}$ -PSMA has a greater sensitivity for disease detection than choline-PET/CT in patients with biochemical recurrence, especially at low PSA values [12, 44]. The ability of PSMA PET/CT to evaluate therapy response has not been systematically evaluated.

### Whole-body MRI (WB-MRI)

Several meta-analyses have shown improved bone and soft tissue disease detection performance of WB-MRI comparable with  $^{18}\text{F}$ -FDG PET/CT, both being

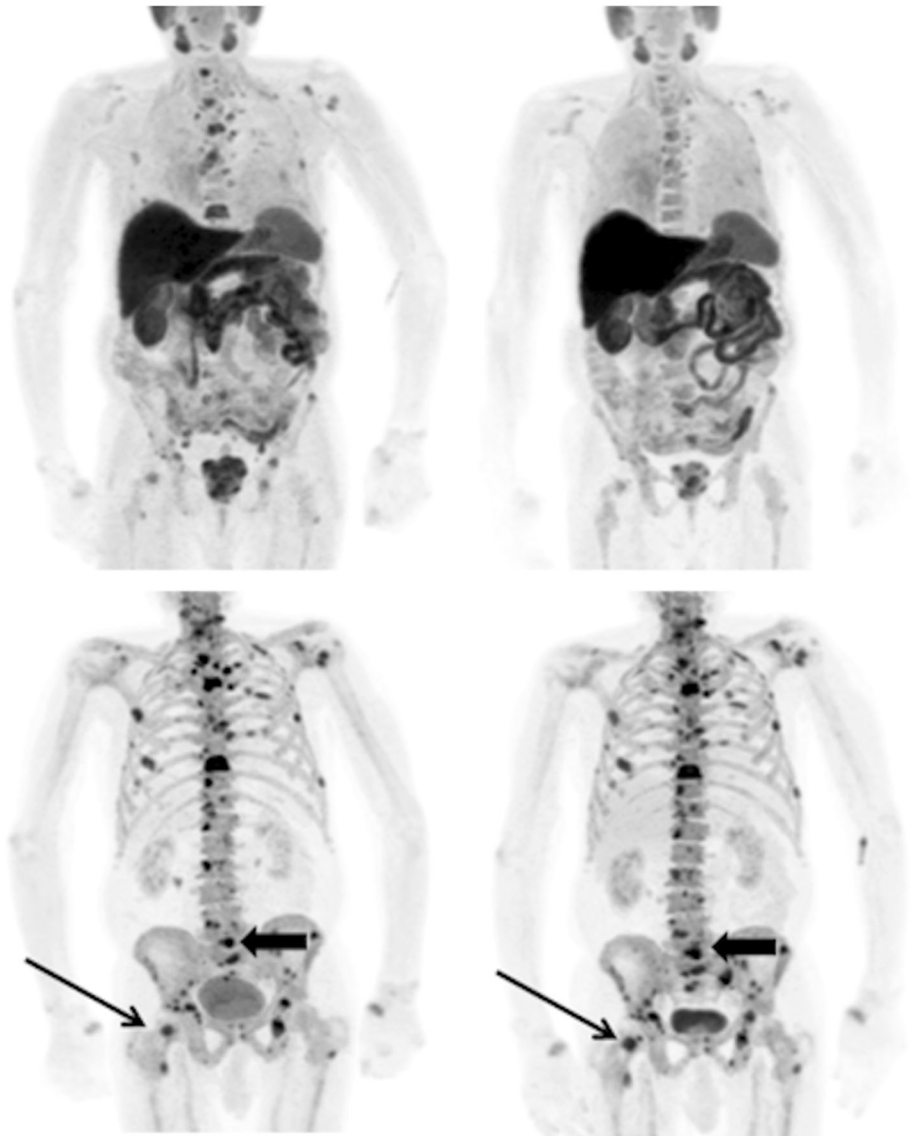
significantly more accurate than bone scans and CT, in the majority of solid cancers, on a per patient and per lesion basis [45–48]. The improved test performance of WB-MRI applies to skeletal assessments in advanced prostate cancer specifically, when choline PET/CT is used as the comparator technique. Shen et al. conducted a meta-analysis of 27 studies in advanced prostate cancer and showed that MRI was superior to choline PET/CT and BS on a per-patient basis [46]. On a per-patient basis, the pooled sensitivities for bone disease using choline PET/CT, WB-MRI and BS were 91 % (95 % CI 83–96), 97 % (95 % CI 91–99) and 79 % (95 % CI 73–83), respectively. The pooled specificities for bone metastases detection using choline PET/CT, WB-MRI and BS were 99 % (95 % CI 93–100), 95 % (95 % CI 90–97) and 82 % (95 % CI 78–85), respectively. On a per-lesion analysis, choline PET/CT had a higher diagnostic odds ratio which exceeded both BS and bone SPECT for detecting bone metastases. Recent studies indicate that diffusion sequences contribute strongly to the enhanced diagnostic capability of WB-MRI. For example, Liu et al. [47] evaluated 32 studies with 1507 patients and showed a pooled sensitivity, specificity and the area under the curve for DWI of 95 % (95 % CI 90–97), 92 % (95 % CI 88–95) and 0.98 on a per-patient basis and 91 % (95 % CI 87–94), 94 % (95 % CI 90–96) and 0.97 on a per-lesion basis.

## Response assessment

### Bone scans

Bone metastases are notoriously difficult to assess for treatment response. RECIST1.1 does not fully cater for response assessment in bone, particularly with sclerotic metastases, and therefore, the Prostate Cancer Working Clinical Trials Group (PCWG) devised a framework specifically for prostate cancer response assessment with a focus on clinical trials [48, 49]. The criteria only allow for progressive disease, i.e. for patients in whom therapy needs to be changed or taken off trial. Bone scintigraphy is considered the standard imaging test and two new lesions are required on follow-up scans to determine progression as long as two new additional lesions are subsequently seen at least 6 weeks later. This is to control for false positives caused by a flare. PCWG recognises that there may be heterogeneity in response between metastases and also recognises alternative imaging methods, including  $^{18}\text{F}$ -fluoride PET,  $^{18}\text{F}$ -FDG PET,  $^{18}\text{F}$ -choline PET and bone marrow/body MRI, but that these should be considered as new biomarkers and are subject to independent validation (see Figs. 1, 2).

**Fig. 1** A patient with metastatic prostate cancer undergoing treatment with docetaxel chemotherapy. Top row  $^{11}\text{C}$ -choline PET maximum intensity projection images at baseline (*left*) and 8 weeks (*right*) and bottom row corresponding  $^{18}\text{F}$ -fluoride PET images. The higher contrast between metastases and the normal skeleton on the  $^{18}\text{F}$ -fluoride scans compared to the  $^{11}\text{C}$ -choline scans allows easier detection of disease. However, whilst there is a clear metabolic response in the bone metastases on the  $^{11}\text{C}$ -choline scans, there is a similar distribution and intensity of most lesions on the  $^{18}\text{F}$ -fluoride scans and some lesions show an increase in activity (arrows). This is likely to be due to a flare response at 8 weeks on the  $^{18}\text{F}$ -fluoride PET scans limiting the sensitivity and specificity in response prediction at early time points with this tracer as changes in osteoblastic activity lag behind changes in tumour metabolism



### $^{18}\text{F}$ -fluoride PET

It is likely that the flare phenomenon will hamper response assessment in bone metastases given the similar mode of uptake to bone scan agents [50]. However, two small studies have shown changes in  $^{18}\text{F}$ -fluoride activity following specific treatments, including  $^{223}\text{Ra}$ -chloride [51] and dasatinib [52]. Total tumour burden measured on baseline  $^{18}\text{F}$ -fluoride PET has also been found to be a predictor of survival and skeletal related events in patients subsequently treated with  $^{223}\text{Ra}$ -chloride [53]. In an interesting case report, a corresponding appearance of progressive disease was seen on both  $^{18}\text{F}$ -fluoride and  $^{68}\text{Ga}$ -PSMA PET/CT following six cycles of  $^{223}\text{Ra}$ -chloride therapy [54]. In a National Oncologic PET Registry study on the effects of  $^{18}\text{F}$ -fluoride PET/CT on monitoring of

systemic cancer therapy (68 % of patients with prostate cancer, 1940 scans), a change in management was recorded in 42 % of patients [55].

### $^{18}\text{F}$ -FDG PET

Whilst metastases from prostate cancer are characteristically not very  $^{18}\text{F}$ -FDG avid, dedifferentiated disease in castrate resistant prostate cancer (CRPC) may show increased glycolytic activity. It has been reported that changes in  $^{18}\text{F}$ -FDG uptake correctly categorised 20/22 patients being treated with an antimicrotubule agent at 4 weeks compared with PCWG PSA criteria [56]. It was found that a 33 % increase in SUVmax or the appearance of a new lesion optimally divided progressors from non-progressors.

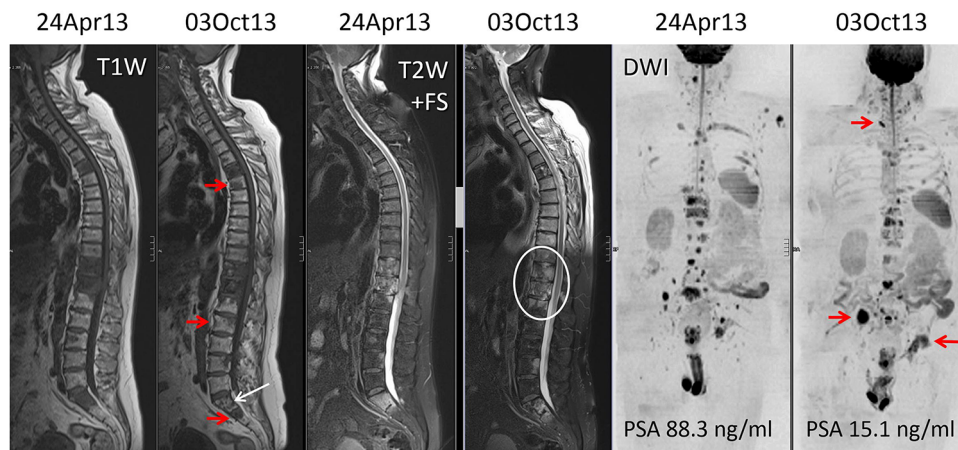


**Fig. 2** A 64 year old man with metastatic castrate resistant prostate cancer. WB-MRI assessments before and after five cycles of abiraterone therapy. The panel pairs are morphologic T1-weighted (*left*) and fat-suppressed T2-weighted (*middle*) sequences, and high *b* value ( $b$  900  $s/mm^2$ ) diffusion-weighted images (*right*) displayed as inverted MIP images. There is a discordant response to therapy

documented on the imaging despite reductions in serum PSA levels. The *white arrows* and *ring* show decrease in tumour in the sacrum with return of normal marrow fat and relief of the spinal cord compression on the fat-suppressed T2-weighted sequence. However, the *red arrows* show disease progression in the spine, right iliac bone and *left acetabulum*

### $^{18}F/^{11}C$ -choline PET

There is a surprising lack of data on the use of PET choline tracers in assessing treatment response in bone metastases given the relatively high sensitivity for detection of disease. This use is supported by preclinical data showing reductions in  $^{11}C$ -choline activity in PC3 xenografts following treatment with docetaxel as soon as 1 week after commencing therapy [57]. Initial data in man are slightly conflicting. In a recent study,  $^{11}C$ -choline PET/CT changes between baseline and after completing treatment with docetaxel were found useful in identifying progression despite an apparent PSA response in a subset of patients [58]. A relationship between changes on  $^{18}F$ -choline PET activity and circulating cell-free DNA has been reported in a small series of eight patients, the authors concluding that the inter-related measures are potential markers of therapeutic response in CRPC [59]. In determining response to enzalutamide, one study showed that only baseline SUVmax of  $^{18}F$ -choline PET was a predictor of PFS and OS [60], whilst another reported that  $^{18}F$ -choline PET/CT does not add more information on OS than PSA alone [61]. In contrast, early  $^{18}F$ -choline PET/CT (3 and 6 weeks) has been reported to be able to predict clinical outcome in CRPC following abiraterone therapy beyond PSA response [62]. The potential value of  $^{18}F$ -choline has been described in two patients receiving  $^{223}Ra$ -chloride therapy with a reduction in lesion SUVs as well as in tumour burden parameters in a responding patient and heterogeneous response in a second patient [63].

### WB-MRI

Morphologic sequences are key for the confident detection of new metastases until the time when diffuse disease occurs after which the detection of disease reactivation becomes problematic. Morphologic criteria for bone disease progression and response are well described in the literature [64]. Specific clinical data on the use of morphological MRI in the routine assessment of metastatic bone disease response in advanced prostate cancer are lacking [65]. There are a number of problems encountered when using morphologic MRI to assess response, which includes arrested resolution of abnormalities despite effective therapy (the ‘residual scar’ phenomenon). Another limitation is the problem of evaluating disease activity on a scarred background of previously treated disease. A “T1 W image pseudoprogession—flare phenomenon” can also occur because of intense bone marrow oedema following tumour cell kill and inflammation, but its frequency is undocumented.

Both preclinical and small-scale clinical studies indicate that diffusion MRI can be useful for the assessment of therapy response in malignant bone marrow disease in prostate cancer. Preclinical mouse model studies of osseous prostate cancers have shown increases in diffusivity values with therapeutic success [66–68]. However, there have been a few systematic studies in prostate cancer patients with bone disease in the response assessment setting [69, 70]. The study of Reischauer et al. found that mean diffusivity of lesions increased significantly after hormonal therapy in keeping with successful

responses gauged by PSA declines [69]. Interestingly, there was also noticeable spatial heterogeneity within individual metastases, with the centre of the lesions having greater increases in water diffusivity as well as variations between metastases in individual patients. Similar findings in bone disease have been described for multiple myeloma, myeloproliferative diseases, breast cancers and primary bone tumours with a variety of treatments, indicating that bone tumour diffusivity increases with successful treatments, and is a generic finding [71–74].

## Conclusion and future directions

There is no doubt that modern imaging methods, including PET/CT with bone-specific and tumour-specific tracers and WB-MRI with DWI, can improve both detection and therapy response assessment of patients with skeletal metastases from prostate cancer. However, it is not yet proved that earlier and more accurate detection of tumour presence and load will have positive therapy implications. It is also not clear that better categorisation of bone metastases response to therapy will have positive benefits. Nevertheless, there are strong indications that more accurate assessments of therapy response (including heterogeneity of response) could further aid the rational development of targeted therapies.

To address these questions, there is a strong need to standardise the evaluation, interpretation and reporting of PET/CT and WB-MRI technologies. By improving the evaluation of metastatic disease presence, load and response, a more complete characterisation of the metastatic state can be obtained, not only at the start of treatment, but also over time as the disease evolves. Whole-body PET/CT and WB-MRI technologies would also enable the evaluation of the benefits of continuing therapy, when there are signs that the disease is progressing. Neither PET/CT nor WB-MRI is at the point where they can support regulatory approvals of new therapeutic approaches in prostate cancer. Thus, we recommend that choline and PSMA PET/CT and WB-MRI are now evaluated in clinical trials to assess their impact on the clinical management of advanced prostate cancer patients.

**Acknowledgments** The authors acknowledge support from the National Institute for Health Research Biomedical Research Centre of Guys and St Thomas' NHS Trust in partnership with Kings College London and also the King's College London and University College London Comprehensive Cancer Imaging Centre funded by Cancer Research UK and the Engineering and Physical Sciences Research Council in association with the Medical Research Council and Department of Health (England) and a research grant from Prostate Cancer UK.

## Compliance with ethical standards

This study does not contain any studies with human or animal subjects performed by any of the authors.

**Conflict of interest** Gary Cook, Gurdip Azad and Anwar Padhani do not have any conflicts of interest.

**Open Access** This article is distributed under the terms of the Creative Commons Attribution 4.0 International License (<http://creativecommons.org/licenses/by/4.0/>), which permits unrestricted use, distribution, and reproduction in any medium, provided you give appropriate credit to the original author(s) and the source, provide a link to the Creative Commons license, and indicate if changes were made.

## References

- Halabi S, Kelly WK, Ma H et al (2016) Meta-Analysis evaluating the impact of site of metastasis on overall survival in men with castration-resistant prostate cancer. *J Clin Oncol* 34:1652–1659
- Coleman RE (2011) Bone cancer in 2011: prevention and treatment of bone metastases. *Nat Rev Clin Oncol* 9:76–78
- Hoefeler H, Duran I, Hechmati G et al (2014) Health resource utilization associated with skeletal-related events in patients with bone metastases: results from a multinational retrospective—prospective observational study—a cohort from 4 European countries. *J Bone Oncol* 3:40–48
- Eisenhauer EA, Therasse P, Bogaerts J et al (2009) New response evaluation criteria in solid tumours: revised RECIST guideline (version 1.1). *Eur J Cancer* 45:228–247
- Paget S (1889) The distribution of secondary growths in cancer of the breast. *Lancet* 89:571
- Ibrahim T, Flamini E, Mercatali L, Sacanna E, Serra P, Amadori D (2010) Pathogenesis of osteoblastic bone metastases from prostate cancer. *Cancer* 15:1406–1418
- Challapalli A, Aboagye EO (2016) Positron emission tomography imaging of tumor cell metabolism and application to therapy response monitoring. *Front Oncol* 29(6):44
- Leisser A, Pruscha K, Ubl P et al (2015) Evaluation of fatty acid synthase in prostate cancer recurrence: SUV of [(11)C]acetate PET as a prognostic marker. *Prostate* 75:1760–1767
- Ren J, Yuan L, Wen G, Yang J (2016) The value of anti-1-aminocyclohexane-1-carboxylic acid PET/CT in the diagnosis of recurrent prostate carcinoma: a meta-analysis. *Acta Radiol* 57:487–493
- Højlund-Carlsen PF, Poulsen MH, Petersen H, Hess S, Lund L (2014) FDG in urologic malignancies. *PET Clin* 9:457–468
- Beattie BJ, Smith-Jones PM, Hanwar YS et al (2010) Pharmacokinetic assessment of the uptake of 16beta-18F-fluoro-5alpha-dihydrotestosterone (FDHT) in prostate tumors as measured by PET. *J Nucl Med* 51:183–192
- Afshar-Oromieh A, Zechmann CM, Malcher A et al (2014) Comparison of PET imaging with a (68)Ga-labelled PSMA ligand and (18)F-choline-based PET/CT for the diagnosis of recurrent prostate cancer. *Eur J Nucl Med Mol Imaging* 41:11–20
- Rowe SP, Mana-Ay M, Javadi MS et al (2016) PSMA-based detection of prostate cancer bone lesions with (18)F-DCFPyL PET/CT: a sensitive alternative to (99 m)Tc-MDP bone scan and Na(18)F PET/CT? *Clin Genitourin Cancer* 14:e115–e118
- Padhani AR, Koh DM, Collins DJ (2011) Whole-body diffusion-weighted MR imaging in cancer: current status and research directions. *Radiology* 261:700–718

15. Reeder SB, Hu HH, Sirlin CB (2012) Proton density fat-fraction: a standardized MR-based biomarker of tissue fat concentration. *J Magn Reson Imaging* 36:1011–1014
16. Ballon D, Watts R, Dyke JP et al (2004) Imaging therapeutic response in human bone marrow using rapid whole-body MRI. *Magn Reson Med* 52:1234–1238
17. Pollen JJ, Witztum KF, Ashburn WL (1984) The flare phenomenon on radionuclide bone scan in metastatic prostate cancer. *AJR Am J Roentgenol* 142:773e6
18. Wadas TJ, Deng H, Sprague JE et al (2009) Targeting the avb3 integrin for small-animal PET/CT of osteolytic bone metastases. *J Nucl Med* 50:1873–1880
19. Miao W, Zheng S, Dai H et al (2014) Comparison of 99 mTc-3PRGD2 integrin receptor imaging with 99 mTc-MDP bone scan in diagnosis of bone metastasis in patients with lung cancer: a multicenter study. *PLoS ONE* 22(9):e111221
20. Taylor BP, Siddique M, Fogelman I et al (2014) Imaging  $\alpha\beta$ 3 integrin expression in bone metastases from prostate cancer. *Nucl Med Commun* 35:551
21. National Institute for Clinical Excellence Improving Outcomes in Urological Cancer (2002). <https://www.nice.org.uk/guidance/csg2> Accessed 19 Jul 2016
22. O'Sullivan JM, Norman AR, Cook GJ, Fisher C, Dearnaley DP (2003) Broadening the criteria for avoiding staging bone scans in prostate cancer: a retrospective study of patients at the Royal Marsden Hospital. *BJU Int* 92:685–689
23. Van den Wyngaert T, Strobel K, Kampen WU et al (2016) The EANM practice guidelines for bone scintigraphy. *Eur J Nucl Med Mol Imaging*. doi:10.1007/s00259-016-3415-4
24. Venkitaraman R, Cook GJ, Dearnaley DP et al (2009) Does magnetic resonance imaging of the spine have a role in the staging of prostate cancer? *Clin Oncol* 21:39–42
25. Helyar V, Mohan HK, Barwick T et al (2010) The added value of multislice SPECT/CT in patients with equivocal bony metastasis from carcinoma of the prostate. *Eur J Nucl Med Mol Imaging* 37:706–713
26. Cook GJ, Venkitaraman R, Sohaib AS et al (2011) The diagnostic utility of the flare phenomenon on bone scintigraphy in staging prostate cancer. *Eur J Nucl Med Mol Imaging* 38:7–13
27. Blau M, Nagler W, Bender MA (1962) Fluorine-18: a new isotope for bone scanning. *J Nucl Med* 3:332e4
28. Blake GM, Park-Holohan SJ, Cook GJ, Fogelman I (2001) Quantitative studies of bone with the use of 18F-fluoride and 99mTc-methylene diphosphonate. *Semin Nucl Med* 31:28–49
29. Even-Sapir E, Metser U, Mishani E, Lievshitz G, Lerman H, Leibovitch I (2006) The detection of bone metastases in patients with high-risk prostate cancer: 99mTc-MDP Planar bone scintigraphy, single- and multi-field-of-view SPECT, 18F-fluoride PET, and 18F-fluoride PET/CT. *J Nucl Med* 47:287–297
30. Hillner BE, Siegel BA, Hanna L, Duan F, Shields AF, Coleman RE (2014) Impact of 18F-fluoride PET in patients with known prostate cancer: initial results from the National Oncologic PET Registry. *J Nucl Med* 55:574–581
31. Shreve PD, Grossman HB, Gross MD, Wahl RL (1996) Metastatic prostate cancer: initial findings of PET with 2-deoxy-2-[<sup>18</sup>F]fluoro-D-glucose. *Radiology* 199:751–756
32. Yeh SD, Imbriaco M, Larson SM et al (1996) Detection of bony metastases of androgen-independent prostate cancer by PET-FDG. *Nucl Med Biol* 23:693–697
33. Vargas HA, Wassberg C, Fox JJ et al (2014) Bone metastases in castration-resistant prostate cancer: associations between morphologic CT patterns, glycolytic activity, and androgen receptor expression on PET and overall survival. *Radiology* 271:220–229
34. Ceci F, Castellucci P, Graziani T et al (2015) 11C-choline PET/CT identifies osteoblastic and osteolytic lesions in patients with metastatic prostate cancer. *Clin Nucl Med* 40:e265–e270
35. Beheshti M, Vali R, Waldenberger P et al (2010) The use of F-18 choline PET in the assessment of bone metastases in prostate cancer: correlation with morphological changes on CT. *Mol Imaging Biol* 12:98–107
36. Evangelista L, Cimitan M, Zattoni F, Guttilla A, Zattoni F, Saladini G (2015) Comparison between conventional imaging (abdominal-pelvic computed tomography and bone scan) and [(18)F]choline positron emission tomography/computed tomography imaging for the initial staging of patients with intermediate- to high-risk prostate cancer: a retrospective analysis. *Scand J Urol* 49:345–353
37. Poulsen MH, Petersen H, Højlund-Carlson PF et al (2014) Spine metastases in prostate cancer: comparison of technetium-99m-MDP whole-body bone scintigraphy, [(18) F]choline positron emission tomography(PET)/computed tomography (CT) and [(18) F]NaF PET/CT. *BJU Int* 114:818–823
38. Wondergem M, van der Zant FM, van der Ploeg T, Knol RJ (2013) A literature review of 18F-fluoride PET/CT and 18F-choline or 11C-choline PET/CT for detection of bone metastases in patients with prostate cancer. *Nucl Med Commun* 34:935–945
39. Picchio M, Spinapolice EG, Fallanca F et al (2012) [11C]Choline PET/CT detection of bone metastases in patients with PSA progression after primary treatment for prostate cancer: comparison with bone scintigraphy. *Eur J Nucl Med Mol Imaging* 39:13–26
40. Beheshti M, Vali R, Waldenberger P et al (2008) Detection of bone metastases in patients with prostate cancer by 18F fluorocholine and 18F fluoride PET-CT: a comparative study. *Eur J Nucl Med Mol Imaging* 35:1766–1774
41. Langsteger W, Balogova S, Huchet V et al (2011) Fluorocholine (18F) and sodium fluoride (18F) PET/CT in the detection of prostate cancer: prospective comparison of diagnostic performance determined by masked reading. *Q J Nucl Med Mol Imaging* 55:448–457
42. Spick C, Polanec SH, Mitterhauser M et al (2015) Detection of bone metastases using 11C-acetate PET in patients with prostate cancer with biochemical recurrence. *Anticancer Res* 35:6787–6791
43. Pyka T, Okamoto S, Dahlbender M et al (2016) Comparison of bone scintigraphy and (68)Ga-PSMA PET for skeletal staging in prostate cancer. *Eur J Nucl Med Mol Imaging*. doi:10.1007/s00259-016-3435-02016
44. Morigi JJ, Stricker PD, van Leeuwen PJ et al (2015) Prospective Comparison of 18F-Fluoromethylcholine versus 68 Ga-PSMA PET/CT in prostate cancer patients who have rising PSA after curative treatment and are being considered for targeted therapy. *J Nucl Med* 56:1185–1190
45. Yang H-L, Liu T, Wang X-M, Xu Y, Deng S-M (2011) Diagnosis of bone metastases: a meta-analysis comparing <sup>18</sup>FDG PET, CT, MRI and bone scintigraphy. *Eur Radiol* 21:2604–2617
46. Shen G, Deng H, Hu S, Jia Z (2014) Comparison of choline-PET/CT, MRI, SPECT, and bone scintigraphy in the diagnosis of bone metastases in patients with prostate cancer: a meta-analysis. *Skeletal Radiol* 43:1503–1513
47. Liu L-P, Cui L-B, Zhang XX et al (2015) Diagnostic performance of diffusion-weighted magnetic resonance imaging in bone malignancy. *Medicine (Baltimore)* 94:e1998
48. Scher HI, Halabi S, Tannock I et al (2008) Design and end points of clinical trials for patients with progressive prostate cancer and castrate levels of testosterone: recommendations of the Prostate Cancer Clinical Trials Working Group. *J Clin Oncol* 26:1148–1159
49. Scher HI, Morris MJ, Stadler WM et al (2016) Trial design and objectives for castration-resistant prostate cancer: updated recommendations from the prostate cancer clinical trials working group 3. *J Clin Oncol* 34:1402–1418



50. Cook GJ, Taylor BP, Glendenning J et al (2015) Heterogeneity of treatment response in skeletal metastases from breast cancer in 18F-fluoride and 18F-FDG PET. *Nucl Med Commun* 36:515–516
51. Cook GJ, Parker C, Chua S, Johnson B, Aksnes AK, Lewington VJ (2011) 18F-fluoride PET: changes in uptake as a method to assess response in bone metastases from castrate-resistant prostate cancer patients treated with 223Ra-chloride (Alpharadin). *EJNMMI Res* 7:4
52. Yu EY, Duan F, Muzi M et al (2015) Castration-resistant prostate cancer bone metastasis response measured by 18F-fluoride PET after treatment with dasatinib and correlation with progression-free survival: results from American College of Radiology Imaging Network 6687. *J Nucl Med* 56:354–60
53. Etchebehere EC, Araujo JC, Fox PS, Swanston NM, Macapinlac HA, Rohren EM (2015) Prognostic factors in patients treated with 223Ra: the role of skeletal tumor burden on baseline 18F-fluoride PET/CT in predicting overall survival. *J Nucl Med* 56:1177–1184
54. Uprimny C, Kroiss A, Nilica B et al (2015) (68)Ga-PSMA ligand PET versus (18)F-NaF PET: evaluation of response to (223)Ra therapy in a prostate cancer patient. *Eur J Nucl Med Mol Imaging* 42:362–363
55. Hillner BE, Siegel BA, Hanna L, Duan F, Quinn B, Shields AF (2015) 18F-fluoride PET used for treatment monitoring of systemic cancer therapy: results from the National Oncologic PET Registry. *J Nucl Med* 56:222–228
56. Morris MJ, Akhurst T, Larson SM et al (2005) Fluorodeoxyglucose positron emission tomography as an outcome measure for castrate metastatic prostate cancer treated with antimicrotubule chemotherapy. *Clin Cancer Res* 11:3210–3216
57. Krause BJ, Souvatzoglou M, Herrmann K et al (2010) [11C]Choline as pharmacodynamic marker for therapy response assessment in a prostate cancer xenograft model. *Eur J Nucl Med Mol Imaging* 37:1861–1868
58. Ceci F, Castellucci P, Graziani T et al (2016) (11)C-Choline PET/CT in castration-resistant prostate cancer patients treated with docetaxel. *Eur J Nucl Med Mol Imaging* 43:84–91
59. Kwee S, Song MA, Cheng I, Loo L, Tiirikainen M (2012) Measurement of circulating cell-free DNA in relation to 18F-fluorocholine PET/CT imaging in chemotherapy-treated advanced prostate cancer. *Clin Transl Sci* 5:65–70
60. Maines F, Caffo O, Donner D et al (2016) Serial (18)F-choline-PET imaging in patients receiving enzalutamide for metastatic castration-resistant prostate cancer: response assessment and imaging biomarkers. *Future Oncol* 12:333–342
61. De Giorgi U, Caroli P, Scarpi E et al (2015) (18)F-Fluorocholine PET/CT for early response assessment in patients with metastatic castration-resistant prostate cancer treated with enzalutamide. *Eur J Nucl Med Mol Imaging* 42:1276–1283
62. De Giorgi U, Caroli P, Burgio SL et al (2014) Early outcome prediction on 18F-fluorocholine PET/CT in metastatic castration-resistant prostate cancer patients treated with abiraterone. *Oncotarget* 5:12448–12458
63. Miyazaki KS, Kuang Y, Kwee SA (2015) Changes in skeletal tumor activity on (18)F-choline PET/CT in patients receiving (223)radium radionuclide therapy for metastatic prostate cancer. *Nucl Med Mol Imaging* 49:160–164
64. Lecouvet FE, Larbi A, Pasoglou V et al (2013) MRI for response assessment in metastatic bone disease. *Eur Radiol* 23:1986–1997
65. Lecouvet FE, Talbot JN, Messiou C et al (2014) Monitoring the response of bone metastases to treatment with Magnetic Resonance Imaging and nuclear medicine techniques: a review and position statement by the European Organisation for Research and Treatment of Cancer imaging group. *Eur J Cancer* 50:2519–2531
66. Hoff BA, Chughtai K, Jeon YH et al (2012) Multimodality imaging of tumor and bone response in a mouse model of bony metastasis. *Transl Oncol* 5:415–421
67. Rozel S, Galbán CJ, Nicolay K et al (2009) Synergy between anti-CCL2 and docetaxel as determined by DW-MRI in a metastatic bone cancer model. *J Cell Biochem* 107:58–64
68. Graham TJ, Box G, Tunariu N et al (2014) Preclinical evaluation of imaging biomarkers for prostate cancer bone metastasis and response to cabozantinib. *J Natl Cancer Inst* 106:dju033
69. Reischauer C, Froehlich JM, Koh DM et al (2010) Bone metastases from prostate cancer: assessing treatment response by using diffusion-weighted imaging and functional diffusion maps—initial observations. *Radiology* 257:523–531
70. Messiou C, Collins DJ, Giles S et al (2011) Assessing response in bone metastases in prostate cancer with diffusion weighted MRI. *Eur Radiol* 21:2169–2177
71. Messiou C, Giles S, Collins DJ et al (2012) Assessing response of myeloma bone disease with diffusion-weighted MRI. *Br J Radiol* 85:e1198–e1203
72. Hayashida Y, Yakushiji T, Awai K et al (2006) Monitoring therapeutic responses of primary bone tumors by diffusion-weighted image: initial results. *Eur Radiol* 16:2637–2643
73. Ballon D, Watts R, Dyke JP et al (2004) Imaging therapeutic response in human bone marrow using rapid whole-body MRI. *Magn Reson Med* 52:1234–1238
74. Lee KC, Bradley DA, Hussain M et al (2007) A feasibility study evaluating the functional diffusion map as a predictive imaging biomarker for detection of treatment response in a patient with metastatic prostate cancer to the bone. *Neoplasia* 9:1003–1011